Published in final edited form as:
Cell Tissue Res. 2017 June ; 368(3): 487–501. doi:10.1007/s00441-017-2580-5.

Chromogranin A regulates vesicle storage and mitochondrial dynamics to influence insulin secretion

Joshua Wollam[1], **Sumana Mahata**[2], **Matthew Riopel**[1], **Angelina Hernandez-Carretero**[1], **Angshuman Biswas**[1], **Gautam K. Bandyopadhyay**[1], **Nai-Wen Chi**[1,3], **Lee E. Eiden**[4], **Nitish R. Mahapatra**[5], **Angelo Corti**[6], **Nicholas J. G. Webster**[1,3], **Sushil K. Mahata**[1,3,7]

[1]Department of Medicine, University of California, San Diego, La Jolla, CA, USA

[2]Division of Biology & Biological Engineering, California Institute of Technology, Pasadena, CA, USA

[3]VA San Diego Healthcare System, San Diego, CA, USA

[4]Section on Molecular Neuroscience, NIMH-IRP, Bethesda, MD, USA

[5]Department of Biotechnology, Indian Institute of Technology Madras, Chennai 600036, India

[6]IRCCS San Raffaele Scientific Institute, San Raffaele Vita-Salute University, Milan, Italy

[7]Metabolic Physiology & Ultrastructural Biology Laboratory, Department of Medicine, University of California, San Diego (0732), 9500 Gilman Drive, La Jolla, CA 92093-0732, USA

Abstract

Chromogranin A (CgA) is a prohormone and a granulogenic factor that regulates secretory pathways in neuroendocrine tissues. In β-cells of the endocrine pancreas, CgA is a major cargo in insulin secretory vesicles. The impact of CgA deficiency on the formation and exocytosis of insulin vesicles is yet to be investigated. In addition, no literature exists on the impact of CgA on mitochondrial function in β-cells. Using three different antibodies, we demonstrate that CgA is processed to vasostatin- and catestatin-containing fragments in pancreatic islet cells. CgA deficiency in *Chga*-KO islets leads to compensatory overexpression of chromogranin B, secretogranin II, SNARE proteins and insulin genes, as well as increased insulin protein content. Ultrastructural studies of pancreatic islets revealed that *Chga*-KO β-cells contain fewer immature secretory granules than wild-type (WT) control but increased numbers of mature secretory granules and plasma membrane-docked vesicles. Compared to WT control, CgA-deficient β-cells exhibited increases in mitochondrial volume, numerical densities and fusion, as well as increased expression of nuclear encoded genes (*Ndufa9, Ndufs8, Cyc1* and *Atp5o*). These changes in secretory vesicles and the mitochondria likely contribute to the increased glucose-stimulated insulin secretion observed in *Chga*-KO mice. We conclude that CgA is an important regulator for coordination of mitochondrial dynamics, secretory vesicular quanta and GSIS for optimal

✉Sushil K. Mahata smahata@ucsd.edu.
Joshua Wollam and Sumana Mahata contributed equally to this work.

Compliance with ethical standards
Conflict of interest The authors declare that they have no conflict of interest.

secretory functioning of β-cells, suggesting a strong, CgA-dependent positive link between mitochondrial fusion and GSIS.

Keywords

Insulin; Glucagon; Somatostatin; Chromogranin A; Pancreastatin; Catestatin; Dense core vesicle; Mitochondria

Introduction

The major proteins of the chromogranin/secretogranin protein family include the founding member chromogranin A (CgA) as well as chromogranin B (CgB) and secretogranin II (SgII). CgA is implicated in the initiation and regulation of dense core granule (DCG) biogenesis and the sequestration of hormones in neuroendocrine cells (Elias et al. 2012; Iacangelo and Eiden 1995; Kim et al. 2001; Taupenot et al. 2002) and is co-stored and co-secreted with various hormones (Bartolomucci et al. 2011; Winkler and Fischer-Colbrie 1992). CgA is synthesized as a proprotein with multiple dibasic amino acid cleavage sites and gives rise to several biologically active peptides, such as pancreastatin (PST) (Bandyopadhyay et al. 2015; Gayen et al. 2009b; Sanchez-Margalet et al. 2010; Tatemoto et al. 1986), vasostatin (VS1) (Aardal et al. 1993; Tota et al. 2008), catestatin (CST) (Angelone et al. 2008; Mahapatra et al. 2005; Mahata et al. 1997, 2003, 2010) and serpinin (SPN) (Tota et al. 2012). Because of the lack of these peptides, *Chga*-KO mice are hypertensive (Mahapatra et al. 2005) and hyperadrenergic (Mahapatra et al. 2005) and show hepatic insulin sensitivity (Bandyopadhyay et al. 2015; Gayen et al. 2009b) and muscle impairments (Tang et al. 2017).

CgA immunoreactivity has been reported in neuroendocrine cells of the pancreas including glucagon-producing α-cells (Varndell et al. 1985; Wilson and Lloyd 1984), insulinproducing β-cells (O'Connor et al. 1983), somatostatin-producing δ-cells and pancreatic polypeptide-producing cells (Cohn et al. 1984). Immuno-electron microscopy localized CgA in the secretory granules of pancreatic islets (Ehrhart et al. 1986; Lukinius et al. 2003). We previously reported that *Chga*-KO mice are euglycemic despite lower plasma insulin levels than wild-type (WT) mice. This relative hypoinsulinemia was due to enhanced insulin clearance (Gayen et al. 2009b). CgA is processed to PST in insulinoma cells (Arden et al. 1994) and inhibits the 1st phase of insulin response following glucose challenge (Ahren et al. 1996; Efendic et al. 1987; Hertelendy et al. 1996; Ma et al. 1996). Consistent with these reports, we found increased glucose-stimulated insulin secretion (GSIS) in *Chga*-KO mice (Gayen et al. 2009b). The findings of hypoinsulinemia in *Chga*-KO mice along with inhibitory effects of CgA peptides on insulin secretion prompted us to characterize β-cell granules in the pancreas.

Stimulus-secretion coupling has been extensively studied in both chromaffin cells and β-cells. The primary stimulus for catecholamine secretion from the adrenal medulla is acetylcholine, which binds to nicotinic acetylcholine receptor and induces an influx of sodium ions inside the cell causing depolarization of the cell membrane, the opening of voltage-gated Ca^{2+} channels and an influx of Ca^{2+} ions leading to exocytotic secretion of

catecholamines (Mahata et al. 1997). Upon increased splanchnic nerve stimulation under both systemic (hypoglycemic) or psychogenic stress, the primary stimulus for catecholamine secretion is the neuropeptide PACAP (pituitary adenylate cyclase-activating polypeptide), also causing calcium influx and eventuating in exocytotic secretion of catecholamines (Smith and Eiden 2012; Stroth et al. 2013). In β-cells, in contrast, the primary stimulus for insulin secretion is glucose. Mitochondria are the organelle that connects glucose metabolism to exocytotic events (Liesa and Shirihai 2013; Maechler et al. 2006; Park et al. 2008). Export of ATP from the mitochondria to the cytosol induces the closure of the K_{ATP}-channel on the plasma membrane resulting in the depolarization of the cell and the opening of the voltage-gated Ca^{2+} channels (Ashcroft 2006). Increased cytosolic Ca^{2+} is the final necessary signal for exocytotic release of insulin to maintain normal glucose level (Eliasson et al. 2008). We tested the hypothesis whether lack of CgA affected insulin storage and secretion like the ones we reported previously in chromaffin cells of the adrenal medulla. In addition, we sought to determine whether lack of CgA could provide a link between insulin secretion and mitochondrial dynamics.

Indeed, we found that CgA deficiency resulted in compensatory increases in CgB and SgII and increases in insulin 1, insulin 2 and glucagon in pancreatic islets. While WT islets show a preponderance of immature secretory granules (ISG), *Chga*-KO islets are enriched in mature secretory granules (MSG). We also observed increased docked vesicles and expression of SNARE proteins in *Chga*-KO islets. Finally, we report for the first time increased mitochondrial fusion resulting in longer mitochondria in *Chga*-KO mice that may be coupled to increased GSIS.

Materials and methods

Animals

Male (22–24 weeks old) *Chga*-KO mice on a C57BL/6 J background were used in this study. Mice were kept on a 12-h dark/light cycle and fed ad libitum with a normal chow diet (NCD: 14 % calories from fat; LabDiet 5P00). The Institutional Animal Care and Use Committees at the University of California San Diego approved all procedures.

Determination of pancreatic insulin content

Half of the pancreas was dissected out from 12-h fasted mice, put into 5 ml acid-ethanol solution (1.5 % HCl in 70 % ethanol) and kept at −20 °C overnight. Tissues were homogenized using a Polytron homogenizer and kept at −20 °C overnight. Tissues were homogenized again and centrifuged at 2000 rpm at 4 °C. A 100-μl aliquot of the aqueous solution was neutralized with 100 μl of 1 M Tris (pH 7.5). Neutralized samples were diluted (1:1000) with insulin ELISA sample diluent and insulin content measured by ELISA. Insulin content was expressed as ng/μg protein.

Glucose-stimulated insulin secretion *in vivo*

Mice were fasted for 12 h and then injected with glucose (1 mg/g i.p.). Blood (20 μl) was collected from the tail tip using capillary tubes at 0 (before injection of glucose), 7, 15

and 90 min after injection of glucose. Plasma was separated and used for determination of insulin by ELISA.

Isolation of pancreatic islets

Primary murine islets were isolated as previously described (Lee et al. 2013). Briefly, the bile duct was ligated near the ampulla of vater, cannulated and injected with 3 ml of Hanks Buffered Saline Solution containing CIzyme RI collagenase (12,500 CDA U/ml; VitaCyte, USA). The pancreas was dissected from the surrounding tissues, removed and incubated in a shaking bath for 17 min at 37 °C, 200 rpm. The digested tissue was washed with HBSS without collagenase and then the islets were purified by a density gradient (Histopaque 1077 and 1119; Sigma) and centrifuged at 2080 rpm for 18 min. Islets were picked by hand and allowed to recover overnight in DMEM containing 1 g/L glucose and 10 % fetal bovine serum.

Real-time RT-PCR assay for measurement of target mRNAs

Total RNA from isolated pancreatic islets was isolated by using the RNeasy Mini Kit (Qiagen, Valencia, CA, USA) and reverse-transcribed by using the qScript cDNA synthesis kit (Quantabio, Beverly, MA, USA). cDNA samples were amplified by using PERFECTA SYBR FASTMIX L-ROX 1250 (Quantabio) and analyzed on an Applied Biosystems 7500 Fast Real-Time PCR system (Foster City, CA, USA). All PCRs were normalized to *Gapdh* and relative expression levels were determined by the $\Delta\Delta C_t$ method. Primer sequences are provided in Table 1.

Transmission electron microscopy (TEM)

Mice were deeply anesthetized and the pancreas was perfusion-fixed through the left ventricle. Mice were flushed with a pre-warmed (37 °C) calcium- and magnesium-free buffer for 3 min followed by perfusion with freshly prepared pre-warmed (37 °C) fixative containing 2.5 % glutaraldehyde and 2 % paraformaldehyde in 0.15 M cacodylate buffer for 3 min (5 ml/min) using a peristaltic pump (Langer Instruments; Boonton, NJ, USA) as described previously (Pasqua et al. 2016). The pancreas was dissected out, cut into small pieces (2 mm thick), put in the same fixative overnight (2 h at room temperature and 12 h at 4 °C) and postfixed in 1 % OsO_4 in 0.1 M cacodylate buffer for 1 h on ice. The tissues were stained en bloc with 2–3 % uranyl acetate for 1 h on ice. The tissues were dehydrated in graded series of ethanol (20–100 %) on ice followed by one wash with 100 % ethanol and two washes with acetone (15 min each) and embedded with Durcupan. Sections were cut at 50–60 nm on a Leica UCT ultramicrotome and picked up on Formvar and carbon-coated copper grids. Sections were stained with 2 % uranyl acetate for 5 min and Sato's lead stain for 1 min. Grids were viewed using a JEOL 1200EX II (Peabody, MA, USA) TEM and photographed using a Gatan digital camera (Gatan, Pleasanton, CA, USA). Grids were also viewed using an FEI Tecnai Spirit G2 BioTWIN Transmission Electron Microscope and photographed with a bottom mount Eagle 4 k (16 megapixel) camera (Hillsboro, OR, USA). Toluidine blue-stained semi-thin (1 μm) sections were photographed using an Axio Observer Stand Mot microscope (Carl Zeiss Microscopy; Thornwood, NY, USA). Micrographs were randomly taken from 4 pancreases each from WT and *Chga*-KO mice, which were fixed and processed on two different days.

Morphometric analysis

To minimize the bias measurements, samples were blinded and two people performed measurements randomly from different cells. The line segment tool in ImageJ was used to measure diameters (ISG, MSG, ISGC and MSGC) and length (mitochondria). The free-hand tool was used to manually trace around the granule membrane (ISG and MSG) and core (ISGC and MSGC) area. For determination of the volume density (%) of vesicles, the sum of the area of the vesicles was divided by the area of the cytoplasm and multiplied by 100 as described previously (Mahata et al. 2016).

Western blotting

Isolated pancreatic islets were homogenized in a RIPA buffer containing phosphatase and protease inhibitors. Homogenates were subjected to SDS-PAGE (10–12 %), transferred to a PVDF membrane and immunoblotted with polyclonal α-CST ($CgA_{352–372}$) (Pasqua et al. 2016) and α-C-terminal (CT)-CST ($CgA_{368–373}$) (Bianco et al. 2016) and monoclonal α-VS1 ($CgA_{47–57}$) antibodies (Colombo et al. 2002; Ratti et al. 2000).

Data presentation and statistical analysis

Data are expressed as mean ± SEM. Statistical analyses were performed using Student's *t* tests, Kolmogorov-Smirnov test as well as 2-way ANOVA followed by Dunnett's post hoc test when appropriate. Statistical significance was defined as $P < 0.05$. Statistics were computed with the software package, Prism 7 (GraphPad Software; San Diego, CA, USA).

Results

CgA is expressed in murine pancreatic islets and influences the vesicular quanta

To investigate the function of CgA in pancreatic islets, we first measured expression of CgA and its proteolytic fragments in isolated murine islets using three antibodies: polyclonal α-CST ($CgA_{352–372}$) (Pasqua et al. 2016) detecting full-length CgA, monoclonal α-VS1 ($CgA_{47–57}$, mAb 5A8) (Colombo et al. 2002; Ratti et al. 2000) and α-CT (C-terminal)-CST ($CgA_{368–373}$) (Bianco et al. 2016). In the WT islets, α-CST antibody detected CgA at ~75 kDa (Fig. 1a). α-VS1 showed only a VS-1 containing a ~18-kDa fragment (Fig. 1b), while α-CT-CST detected a ~65-kDa and a ~20-kDa fragment (Fig. 1c). All three antibodies demonstrate the ablation of CgA and its processed products in *Chga*-KO islets (Fig. 1a–c). We reasoned that a lack of CgA, a granulogenic protein and a modulator of vesicular quanta in other secretory cells (Kim et al. 2001; Montesinos et al. 2008; Pasqua et al. 2016; Taupenot et al. 2002), might impact vesicle numbers in pancreatic islets. *Chga*-KO islets show significantly higher insulin content compared to WT islets (Fig. 1d). The mRNA levels of the vesicular proteins such as *Chga* (chromogranin A), *Chgb* (chromogranin B), *Scg2* (secretogranin II), *Ins1* (insulin 1), *Ins2* (insulin 2), *Gcg* (glucagon) and *Sst* (somatostatin) in WT islets are shown in Fig. 1e. As expected, *Chga* mRNA is not detected in *Chga*-KO islets (Fig. 1f) but these islets show increased expression of vesicular secretory proteins such as *Chgb* (Fig. 1g) and *Scg2* (Fig. 1h) consistent with a compensatory increase to maintain the vesicular quanta, as well as increased *Ins1* (Fig. 1i), *Ins2* (Fig. 1j) and *Gcg* (Fig. 1k) but not *Sst* (Fig. 1l).

CgA does not influence ontogenesis or differentiation of pancreatic islets

Another mechanism by which islet function can be altered is through changes in embryonic development of the pancreas. In adult pancreatic islets, the expression of ontogenesis and differentiation transcription factor genes such as *Mafa, Pdx1*, *Ngn3* and *Pax4* were comparable between WT and *Chga*-KO mice, as shown in Fig. 2a. Knockout of the *Chga* gene does not affect the expression of any of these transcription factors (Fig. 2b–e). Consistent with gene expression data, we found comparable pancreatic islet size in WT (Fig. 2f) and *Chga*-KO (Fig. 2g) mice. Thus, lack of *Chga* does not lead to a change in islet differentiation and development.

Analysis of α, β and δ-cell vesicular structure in pancreatic islets

As a lack of CgA leads to changes in islet vesicular protein expression, we utilized TEM to analyze the structure of vesicles in different cell types of the islet. At the ultrastructural level, α-cells (glucagon-producing) are easily distinguished by the presence of round dense core vesicles without any halo (Fig. 2h, i). In contrast, β-cells (insulin-producing) are characterized by the presence of immature secretory granules (ISG) with light core as well as mature secretory granules (MSG) with a dense core and a prominent halo (Fig. 2j–m) (Alarcon et al. 2016). Note an ISG visible at the tip of a Golgi stack in a *Chga*-KO islet (Fig. 2m). δ-cells (somatostatin-producing) are characterized by the presence of irregular-shaped vesicles with a light core (Fig. 2n, o) (Alarcon et al. 2016).

CgA deficiency leads to increased size and maturation of β-cell secretory granules

The diameter of ISGs ranges from 150 to 450 nm (mean 290 nm) in WT islets and from 150 to 700 nm (mean 365 nm) in *Chga*-KO islets (Fig. 3a–d), a highly significant difference (Kolmogorov-Smirnov D = 0.31; $P < 0.0001$). ISG core (ISGC) diameters in WT mice range from 150 to 400 nm (mean 259 nm) compared to 150–700 nm (mean 337 nm) in *Chga*-KO islet (Fig. 3a, b, d). ISGC diameters show a similar increase in *Chga*-KO islets (Kolmogorov-Smirnov D = 0.35; $P < 0.0001$). There was a marked decrease in abundance of ISG in *Chga*-KO islets (Fig. 3e). MSG diameters in WT islets range from 150 to 500 nm (mean 217 nm) compared to 150–1,000 nm (mean 269 nm) in *Chga*-KO islets (Fig. 3f–h). MSG diameters in *Chga*-KO islets are significantly larger than WT islets (Kolmogorov-Smirnov D = 0.38; $P < 0.0001$). In WT islets, MSG Core (MSGC) diameters range from 100–300 nm (mean 217 nm) compared to 100–550 nm (mean 269 nm) in *Chga*-KO islets (Fig. 3f, g, i). Like ISGC diameters, MSGC in *Chga*-KO islets are larger than WT controls (Kolmogorov-Smirnov D = 0.39; $P < 0.0001$). In sharp contrast to ISV, *Chga*-KO mice show a marked increase in the abundance of MSG (Fig. 3j), indicating an effect on vesicle maturation. So, CgA deficiency appears to promote maturation and increased packaging of insulin vesicles.

CgA influences mitochondrial morphology and abundance in β-cells

Since mitochondria play a central role in glucose-stimulated insulin secretion, we analyzed morphometry of mitochondria. *Chga*-KO islets show a significant increase in mitochondrial abundance, fractional volume and area (Fig. 4a–d). In WT islets, the mitochondrial area ranges from 25 to 550 nm^2 (mean 117 nm^2) compared to 50–650 nm^2 (mean 154 nm^2) in

Chga-KO islets (Fig. 4e). Statistical analysis revealed a highly significant shift in the size distribution towards larger the mitochondrial area in *Chga*-KO islet (Kolmogorov-Smirnov D = 0.21; $P < 0.0001$). Mitochondrial length in WT islets range from 150 to 1250 nm (mean 532 nm) compared to 200–1900 nm (mean 592 nm) in *Chga*-KO islets (Fig. 4f). Statistical analysis also showed a shift in the distribution of mitochondrial lengths towards longer mitochondria (Fig. 4f).

CgA deficiency leads to augmented exocytosis and elevated glucose-stimulated insulin secretion (GSIS)

We found the insulin content in *Chga*-KO mice to be increased in the pancreas but decreased in the plasma (Fig. 5a, b). These mice displayed ~120–150 % increase in insulin levels after 7 and 15 min of glucose infusion compared to WT mice. We observed increased expression of multiple SNARE proteins involved in exocytosis, including *Vamp1* (a v-SNARE), *Stx1a* (Syntaxin 1a, a t-SNARE) and *Snap25* (synaptosomal-associated protein 25 kDa, a t-SNARE) (Fig. 5j–m). The increased SNARE protein expression correlated with a greater number of docked MSG at the plasma membrane, exocytosis and endocytosis in *Chga*-KO mice (Fig. 5e–i).

CgA modulates the expression of genes regulating mitochondrial function

As mitochondrial activities influence exocytosis, we investigated the expression of genes regulating mitochondrial function. Multiple proteins encoded by either the mitochondrial genome or the nuclear genome regulate mitochondrial function. Western blot analyses of *Chga*-KO islets revealed decreased expression of nuclear-encoded *Ndufb8* (NADH-ubiquinone oxidoreductase 1 beta subcomplex 8), *Sdhb* (succinate dehydrogenase complex subunit B), *Uqcrc2* (ubiquinol-cytochrome c reductase core protein II) and *Atp5a* (ATP synthase H^+ transporting mitochondrial F1 complex alpha subunit 1) compared to WT islets (Fig. 6a). The expression of mitochondria-encoded genes such as *mtCo1* (complex IV cytochrome c oxidase subunit 1), *mtAtp6* (ATP synthase 6), *mtNd1* (complex I subunit Nd1), *mtNd2* (complex I subunit Nd2) and *mtCyb* (cytochrome b of complex III) was comparable between WT and *Chga*-KO islets (Fig. 6b–g). In contrast, nuclear-encoded complex I genes such as *Ndufa9* (NADH-ubiquinone oxidoreductase 1 alpha subcomplex 9) and *Ndufs8* (NADH-ubiquinone oxidoreductase Fe-S protein 8) were higher in *Chga*-KO islets but the complex II gene *Sdhb* was lower while *Ndufv2* and *Sdha* were comparable (Fig. 6h–m). Amongst the complex III genes, *Cyc1* (cytochrome c1) was increased but *Uqcrc2* decreased and the complex V gene *Atp5a1* was increased (Fig. 6n–s) between *Chga*-KO and WT mice.

Chga-KO islets display altered mitochondrial dynamics

At the ultrastructural level, *Chga*-KO islets displayed longer linear mitochondria (Fig. 7b) as well as tubular networks (Fig. 7c, d), implicating mitochondrial fusion. We were able to capture mitochondria after fusion (Fig. 7b, c) and undergoing fusion (Fig. 7d). The *Chga*-KO islet showed reduced expression of *Park2* (Fig. 7f), a mediator of mitophagy. In line with the ultrastructural findings, *Chga*-KO islets showed increased expression of fusion genes *Opa1* (Fig. 7n), *Mfn1* (Fig. 7o) and *Mfn2* (Fig. 7p). Expression of other genes such as the mitophagy gene *Pink1* (PTEN-induced putative kinase 1; Fig. 7g), fission genes *Drp1*

(Fig. 7h), *Mff* (Fig. 7i), biogenesis genes *Tfam* (mitochondrial transcription factor A; Fig. 7j), *Nrf1* (Fig. 7k), *Nrf2* (nuclear respiratory factor 2; Fig. 7l) and *Pgc1α* (peroxisome proliferator-activated receptor-γ coactivator-1α; Fig. 7m) is comparable between WT and *Chga*-KO islets.

Discussion

It is well established that CgA plays a pivotal role in the initiation and regulation of dense core secretory granule biogenesis and hormone sequestration in neuroendocrine cells (Elias et al. 2012; Iacangelo and Eiden 1995; Kim et al. 2001; Taupenot et al. 2002). In chromaffin granules of the adrenal medulla, we reported that lack of CgA resulted in a compensatory increase in mRNA levels of the other secretogranins *Chgb* and *Scg2* (Mahapatra et al. 2005). Here, in pancreatic β-cells, we found that lack of CgA resulted in a compensatory increase in *Chgb* and *Scg2* along with increased expression of the *Ins1*, *Ins2* and *Gcg* genes. These changes may be compensatory, serving to maintain proper vesicular quanta. In chromaffin cells, loss of CgA causes decrease in catecholamine content, suggesting that CgB and SgII cannot compensate completely for the catecholamine binding activity of CgA. In contrast, loss of CgA in β-cells resulted in higher insulin content and larger ISG and MSG. This is perhaps because insulin is not only co-stored with CgA but, unlike catecholamines, also depends on prohormone production coupled to secretory vesicle packaging and processing. In addition, *Chga*-KO islets show increased populations of MSG. Of note, the total number of vesicles (ISG plus MSG) is comparable between WT and *Chga*-KO pancreas. Based on CgA's role in protein trafficking (Taupenot et al. 2002), it was expected that post-translational stabilization of granule proteins in the Golgi complex could not happen properly in CgA-deficient β-cells but that did not hinder budding of defective ISGs carrying mis-sorted proteins. Extensive clean-up operations directed to removing surface clathrin molecules and mis-sorted proteins were there to clear the ISGs in lysosomes of *Chga*-KO cells (thus reducing their number per unit area). Eventually, functional MSGs emerged. Thus, CgA appears to affect granulogenesis in both chromaffin cells and β-cells. Interestingly, a lack of CgA induces increased hormone secretion in both chromaffin and β-cells. However, CgA acts to promote episodic regulated secretion in chromaffin cells but also to modulate constant ongoing regulated secretion in β-cells. Thus, in chromaffin cells, increased basal catecholamine secretion results from CgA deficiency (Montesinos et al. 2008; Pasqua et al. 2016), whereas, in β-cells, regulated secretion is inappropriately upregulated in the absence of CgA. However, we identified an additional role for CgA in β-cells: a role in modulating via effects on mitochondrial dynamics (vide infra) affecting ATP production, the subsequent glucose-stimulated insulin secretion.

The implications of these findings are also worthy of consideration for understanding the role of CgA in maintaining the regulated secretory state in neuroendocrine cells in general. CgA is 'granulogenic' in chromaffin cells (Elias et al. 2012; Iacangelo and Eiden 1995; Kim et al. 2001; Taupenot et al. 2002) and its deletion results in both a decrease in the number of mature secretory vesicles in that tissue (Kim et al. 2005; Mahapatra et al. 2005; Pasqua et al. 2016) and a decrease in the efficiency of biogenic amine storage (Montesinos et al. 2008; Pasqua et al. 2016). There is, however, a robust compensation in VMAT2-mediated *overall* biogenic amine storage, linked to mitochondrial alterations

leading to enhanced energy expenditure, such that epinephrine is available for secretion even during periods of enhanced release, such as following elicitation of splanchnic nerve firing by hypoglycemic shock (Pasqua et al. 2016). Furthermore, systemic effects of CgA deficiency, including hypertension (Gayen et al. 2009a, 2010; Mahapatra et al. 2005) and hypoinsulinemia (Bandyopadhyay et al. 2015; Gayen et al. 2009b), due to dysfunction of multiple endocrine secretory systems, are differentially rescued with CgA-derived hormones, including pancreastatin and catestatin. This reflects the pleiotropic role of CgA as both a granulogenic factor and prohormone precursor for factors acting at hormonal, paracrine and autocrine levels. Finally, our current results show that the overall effects of CgA deletion from endocrine cells is dependent on their ability to compensate these granulogenic and hormonal/paracrine/autocrine effects of CgA by upregulation of other granin proteins, including CgB and secretogranin II. Thus, CgA deficiency has highly specific effects on multiple endocrine tissues in which it is expressed. Organ-specific knock-out of CgA will help both to define its organ-specific roles and, more important for translational purposes, how individual failing or dysfunctional endocrine systems might respond to systemic administration of CgA-derived bioactive peptides including pancreastatin (Bandyopadhyay et al. 2015; Gayen et al. 2009b; Sanchez-Margalet et al. 2010; Tatemoto et al. 1986), catestatin (Mahapatra et al. 2005; Mahata et al. 1997, 2003), vasostatin (Aardal et al. 1993; Tota et al. 2008) and serpinin (Tota et al. 2012).

Mitochondria constantly undergo biogenesis, fusion, fission and mitophagy and can change rapidly in response to external insults and metabolic cues. Mitochondrial fusion is regulated by the outer mitochondrial membrane dynamin-related mitofusins (Mfn1 and Mfn2) (Santel and Fuller 2001) and the inner mitochondrial membrane optic atrophy protein 1 (Opa1) (Misaka et al. 2002). Fusion is thought to limit deleterious mutations in mitochondrial DNA (Santel et al. 2003), maximize oxidative phosphorylation (OXPHOS) activity by inducing supercomplexes of the electron transport chain (ETC.) (Cogliati et al. 2013; Mishra et al. 2014) and enhance interaction with the ER, which is important for Ca^{2+} flux. Although extensive fusion of mitochondria represents an adaptation to CgA deficiency, recent studies (Buck et al. 2016; Kakimoto and Kowaltowski 2016) have indicated that such adaptation might elevate mitochondrial bioenergetics and bring in metabolic benefits. Our results also suggest CgA-deficient islets may benefit from increased mitochondrial fusion.

Although fusion/fission events are distinct from mitochondrial bioenergetic pathways, recent studies suggest that metabolism and dynamics are interrelated (Liesa and Shirihai 2013) and that the balance between mitochondrial fusion and fission is crucial to the regulation of mitochondrial energetics (Putti et al. 2015; Wai and Langer 2016). In this scenario, mitochondrial fusion tracks with optimal mitochondrial function (Westermann 2012). This concept is supported by the observation that starvation increases mitochondrial ATP synthesis capacity and causes elongation of the mitochondria in transformed cell lines (Gomes et al. 2011). In addition, elongated mitochondria also tracks with increased ATP production (Mitra et al. 2009; Tondera et al. 2009). In the present study, *Chga*-KO islets with increases in both mitochondrial fusion and GSIS present a novel positive association between the two processes. Since a lack of PST causes insulin sensitivity (Bandyopadhyay et al. 2015; Gayen et al. 2009b), we interpret our observed increased insulin secretion after a glucose challenge in *Chga*-KO mice to the lack of PST (Ahren et al. 1996; Efendic et al.

1987; Hertelendy et al. 1996; Ma et al. 1996), in particular PST released locally within the pancreatic islet itself, modulating insulin secretion in an autocrine/paracrine fashion.

As discussed above, mitochondria play a critical role in β-cell function. Mitochondrial function requires many polypeptides encoded by the mitochondrial genome and nuclear genome. In MIN6 cells, partial depletion of mitochondrial DNA can impair mitochondrial function and decrease insulin secretion (Soejima et al. 1996; Tsuruzoe et al. 1998). In the present study, expression of mitochondria-encoded genes was comparable between WT and *Chga*-KO islets but a number of nuclear-encoded mitochondrial genes *Cyc1, Uqcrc2, Sdhb* and *Atp5o* were altered. Interestingly, these same genes were reported to be upregulated in diet-induced obese liver (Guo et al. 2013). Decreased expression of Ndufa9 protein has been reported in MKR (a transgenic mouse with a dominantnegative IGF-IR in skeletal muscle) islets compared to WT mice (Lu et al. 2008). Increased expression of *Ndufa9* and decreased expression of *Uqcrc2* and *Sdhb* genes and proteins in *Chga*-KO islets, as reported here, may enhance mitochondrial function.

We conclude that CgA deficiency in pancreatic islets leads to (1) increased intracellular insulin levels accompanied with increased expression of the *Ins1* and *Ins2* genes, (2) increased packaging and docking of insulin MSG and (3) elongated mitochondria owing to increased fusion coupled with increased GSIS, establishing a novel role of CgA in pancreatic biology and physiology.

Acknowledgments

Transmission electron microscopy was conducted at the Cellular & Molecular Medicine Electron Microscopy Core Facility at UCSD. Mahata's home equity loan and VMRF's bridge funding supported this work. The Noland Scholarship from Caltech supported SM.

Abbreviations

CgA	Chromogranin A protein
Chga	Mouse chromogranin A gene
Chgb	Mouse chromogranin b gene
Gc	Golgi complex
Gcg	Mouse glucagon gene
Ins1	Mouse insulin 1 gene
Ins2	Mouse insulin 2 gene
ISG	Immature secretory granule
ISGC	ISG core
Mc	Mitochondria
Nc	Nucleus

MSG	Mature secretory granule
MSGC	MSG core
Scg2	Mouse secretogranin II gene
Sst	Mouse somatostatin gene
TEM	Transmission electron microscopy

References

Aardal S, Helle KB, Elsayed S, Reed RK, Serck-Hanssen G (1993) Vasostatins, comprising the N-terminal domain of chromogranin A, suppress tension in isolated human blood vessel segments. J Neuroendocrinol 5:405–412 [PubMed: 8401564]

Ahren B, Bertrand G, Roye M, Ribes G (1996) Pancreastatin modulates glucose-stimulated insulin secretion from the perfused rat pancreas. Acta Physiol Scand 158:63–70 [PubMed: 8876749]

Alarcon C, Boland BB, Uchizono Y, Moore PC, Peterson B, Rajan S, Rhodes OS, Noske AB, Haataja L, Arvan P, Marsh BJ, Austin J, Rhodes CJ (2016) Pancreatic beta-cell adaptive plasticity in obesity increases insulin production but adversely affects secretory function. Diabetes 65:438–450 [PubMed: 26307586]

Angelone T, Quintieri AM, Brar BK, Limchaiyawat PT, Tota B, Mahata SK, Cerra MC (2008) The antihypertensive chromogranin a peptide catestatin acts as a novel endocrine/paracrine modulator of cardiac inotropism and lusitropism. Endocrinology 149:4780–4793 [PubMed: 18535098]

Arden SD, Rutherford NG, Guest PC, Curry WJ, Bailyes EM, Johnston CF, Hutton JC (1994) The post-translational processing of chromogranin A in the pancreatic islet: involvement of the eukaryote subtilisin PC2. Biochem J 298(Pt 3):521–528 [PubMed: 8141763]

Ashcroft FM (2006) K(ATP) channels and insulin secretion: a key role in health and disease. Biochem Soc Trans 34:243–246 [PubMed: 16545085]

Bandyopadhyay GK, Lu M, Avolio E, Siddiqui JA, Gayen JR, Wollam J, Vu CU, Chi NW, O'Connor DT, Mahata SK (2015) Pancreastatin-dependent inflammatory signaling mediates obesity-induced insulin resistance. Diabetes 64:104–116 [PubMed: 25048197]

Bartolomucci A, Possenti R, Mahata SK, Fischer-Colbrie R, Loh YP, Salton SR (2011) The extended granin family: structure, function, and biomedical implications. Endocr Rev 32:755–797 [PubMed: 21862681]

Bianco M, Gasparri AM, Colombo B, Curnis F, Girlanda S, Ponzoni M, Bertilaccio MT, Calcinotto A, Sacchi A, Ferrero E, Ferrarini M, Chesi M, Bergsagel PL, Bellone M, Tonon G, Ciceri F, Marcatti M, Caligaris-Cappio F, Corti A (2016) Chromogranin A is preferentially cleaved into proangiogenic peptides in the bone marrow of multiple myeloma patients. Cancer Res 76:1781–1791 [PubMed: 26869462]

Buck MD, O'Sullivan D, Klein Geltink RI, Curtis JD, Chang CH, Sanin DE, Qiu J, Kretz O, Braas D, van der Windt GJ, Chen Q, Huang SC, O'Neill CM, Edelson BT, Pearce EJ, Sesaki H, Huber TB, Rambold AS, Pearce EL (2016) Mitochondrial dynamics controls T cell fate through metabolic programming. Cell 166:63–76 [PubMed: 27293185]

Cogliati S, Frezza C, Soriano ME, Varanita T, Quintana-Cabrera R, Corrado M, Cipolat S, Costa V, Casarin A, Gomes LC, PeralesClemente E, Salviati L, Fernandez-Silva P, Enriquez JA, Scorrano L (2013) Mitochondrial cristae shape determines respiratory chain supercomplexes assembly and respiratory efficiency. Cell 155:160–171 [PubMed: 24055366]

Cohn DV, Elting JJ, Frick M, Elde R (1984) Selective localization of the parathyroid secretory protein-I/adrenal medulla chromogranin A protein family in a wide variety of endocrine cells of the rat. Endocrinology 114:1963–1974 [PubMed: 6233131]

Colombo B, Longhi R, Marinzi C, Magni F, Cattaneo A, Yoo SH, Curnis F, Corti A (2002) Cleavage of chromogranin A N-terminal domain by plasmin provides a new mechanism for regulating cell adhesion. J Biol Chem 277:45911–45919 [PubMed: 12297497]

Efendic S, Tatemoto K, Mutt V, Quan C, Chang D, Ostenson CG (1987) Pancreastatin and islet hormone release. Proc Natl Acad Sci U S A 84:7257–7260 [PubMed: 2890162]

Ehrhart M, Grube D, Bader MF, Aunis D, Gratzl M (1986) Chromogranin A in the pancreatic islet: cellular and subcellular distribution. J Histochem Cytochem 34:1673–1682 [PubMed: 2878021]

Elias S, Delestre C, Ory S, Marais S, Courel M, Vazquez-Martinez R, Bernard S, Coquet L, Malagon MM, Driouich A, Chan P, Gasman S, Anouar Y, Montero-Hadjadje M (2012) Chromogranin A induces the biogenesis of granules with calcium- and actin-dependent dynamics and exocytosis in constitutively secreting cells. Endocrinology 153:4444–4456 [PubMed: 22851679]

Eliasson L, Abdulkader F, Braun M, Galvanovskis J, Hoppa MB, Rorsman P (2008) Novel aspects of the molecular mechanisms controlling insulin secretion. J Physiol 586:3313–3324 [PubMed: 18511483]

Gayen JR, Gu Y, O'Connor DT, Mahata SK (2009a) Global disturbances in autonomic function yield cardiovascular instability and hypertension in the chromogranin A null mouse. Endocrinology 150:5027–5035 [PubMed: 19819970]

Gayen JR, Saberi M, Schenk S, Biswas N, Vaingankar SM, Cheung WW, Najjar SM, O'Connor DT, Bandyopadhyay G, Mahata SK (2009b) A novel pathway of insulin sensitivity in chromogranin a null mice: a crucial role for pancreastatin in glucose homeostasis. J Biol Chem 284:28498–28509 [PubMed: 19706599]

Gayen JR, Zhang K, Ramachandrarao SP, Mahata M, Chen Y, Kim H-S, Naviaux RK, Sharma K, Mahata SK, O'Connor DT (2010) Role of reactive oxygen species in hyperadrenergic hypertension: biochemical, physiological, and pharmacological evidence from targeted ablation of the chromogranin A gene. Circ Cardiovasc Genet 3:414–425 [PubMed: 20729505]

Gomes LC, Di Benedetto G, Scorrano L (2011) During autophagy mitochondria elongate, are spared from degradation and sustain cell viability. Nat Cell Biol 13:589–598 [PubMed: 21478857]

Guo Y, Darshi M, Ma Y, Perkins GA, Shen Z, Haushalter KJ, Saito R, Chen A, Lee YS, Patel HH, Briggs SP, Ellisman MH, Olefsky JM, Taylor SS (2013) Quantitative proteomic and functional analysis of liver mitochondria from high fat diet (HFD) diabetic mice. Mol Cell Proteomics 12:3744–3758 [PubMed: 24030101]

Hertelendy ZI, Patel DG, Knittel JJ (1996) Pancreastatin inhibits insulin secretion in RINm5F cells through obstruction of G-protein mediated, calcium-directed exocytosis. Cell Calcium 19:125–132 [PubMed: 8689670]

Iacangelo AL, Eiden LE (1995) Chromogranin A: current status as a precursor for bioactive peptides and a granulogenic/sorting factor in the regulated secretory pathway. Regul Pept 58:65–88 [PubMed: 8577930]

Kakimoto PA, Kowaltowski AJ (2016) Effects of high fat diets on rodent liver bioenergetics and oxidative imbalance. Redox Biol 8:216–225 [PubMed: 26826574]

Kim T, Tao-Cheng J, Eiden LE, Loh YP (2001) Chromogranin A, an "on/off" switch controlling dense-core secretory granule biogenesis. Cell 106:499–509 [PubMed: 11525735]

Kim T, Zhang CF, Sun Z, Wu H, Loh YP (2005) Chromogranin A deficiency in transgenic mice leads to aberrant chromaffin granule biogenesis. J Neurosci 25:6958–6961 [PubMed: 16049171]

Lee YS, Morinaga H, Kim JJ, Lagakos W, Taylor S, Keshwani M, Perkins G, Dong H, Kayali AG, Sweet IR, Olefsky J (2013) The fractalkine/CX3CR1 system regulates beta cell function and insulin secretion. Cell 153:413–425 [PubMed: 23582329]

Liesa M, Shirihai OS (2013) Mitochondrial dynamics in the regulation of nutrient utilization and energy expenditure. Cell Metab 17:491–506 [PubMed: 23562075]

Lu H, Yang Y, Allister EM, Wijesekara N, Wheeler MB (2008) The identification of potential factors associated with the development of type 2 diabetes: a quantitative proteomics approach. Mol Cell Proteomics 7:1434–1451 [PubMed: 18448419]

Lukinius A, Stridsberg M, Wilander E (2003) Cellular expression and specific intragranular localization of chromogranin A, chromogranin B, and synaptophysin during ontogeny of pancreatic islet cells: an ultrastructural study. Pancreas 27:38–46 [PubMed: 12826904]

Ma HT, Kato M, Tatemoto K (1996) Effects of pancreastatin and somato-statin on secretagogues-induced rise in intracellular free calcium in single rat pancreatic islet cells. Regul Pept 61:143–148 [PubMed: 8852817]

Maechler P, Carobbio S, Rubi B (2006) In beta-cells, mitochondria integrate and generate metabolic signals controlling insulin secretion. Int J Biochem Cell Biol 38:696–709 [PubMed: 16443386]

Mahapatra NR, O'Connor DT, Vaingankar SM, Hikim AP, Mahata M, Ray S, Staite E, Wu H, Gu Y, Dalton N, Kennedy BP, Ziegler MG, Ross J, Mahata SK (2005) Hypertension from targeted ablation of chromogranin A can be rescued by the human ortholog. J Clin Invest 115:1942–1952 [PubMed: 16007257]

Mahata SK, O'Connor DT, Mahata M, Yoo SH, Taupenot L, Wu H, Gill BM, Parmer RJ (1997) Novel autocrine feedback control of catecholamine release. A discrete chromogranin A fragment is a non-competitive nicotinic cholinergic antagonist. J Clin Invest 100: 1623–1633 [PubMed: 9294131]

Mahata SK, Mahapatra NR, Mahata M, Wang TC, Kennedy BP, Ziegler MG, O'Connor DT (2003) Catecholamine secretory vesicle stimulus-transcription coupling in vivo. Demonstration by a novel transgenic promoter/photoprotein reporter and inhibition of secretion and transcription by the chromogranin A fragment catestatin. J Biol Chem 278:32058–32067 [PubMed: 12799369]

Mahata SK, Mahata M, Fung MM, O'Connor DT (2010) Catestatin: a multifunctional peptide from chromogranin A. Regul Pept 162:33–43 [PubMed: 20116404]

Mahata SK, Zheng H, Mahata S, Liu X, Patel KP (2016) Effect of heart failure on catecholamine granule morphology and storage in chromaffin cells. J Endocrinol 230:309–323 [PubMed: 27402067]

Misaka T, Miyashita T, Kubo Y (2002) Primary structure of a dynamin-related mouse mitochondrial GTPase and its distribution in brain, subcellular localization, and effect on mitochondrial morphology. J Biol Chem 277:15834–15842 [PubMed: 11847212]

Mishra P, Carelli V, Manfredi G, Chan DC (2014) Proteolytic cleavage of Opa1 stimulates mitochondrial inner membrane fusion and couples fusion to oxidative phosphorylation. Cell Metab 19:630–641 [PubMed: 24703695]

Mitra K, Wunder C, Roysam B, Lin G, Lippincott-Schwartz J (2009) A hyperfused mitochondrial state achieved at G1-S regulates cyclin E buildup and entry into S phase. Proc Natl Acad Sci U S A 106:11960–11965 [PubMed: 19617534]

Montesinos MS, Machado JD, Camacho M, Diaz J, Morales YG, Alvarez de la Rosa D, Carmona E, Castaneyra A, Viveros OH, O'Connor DT, Mahata SK, Borges R (2008) The crucial role of chromogranins in storage and exocytosis revealed using chromaffin cells from chromogranin A null mouse. J Neurosci 28:3350–3358 [PubMed: 18367602]

O'Connor DT, Burton D, Deftos LJ (1983) Chromogranin A: immunohistology reveals its universal occurrence in normal polypeptide hormone producing endocrine glands. Life Sci 33:1657–1663 [PubMed: 6633161]

Park KS, Wiederkehr A, Kirkpatrick C, Mattenberger Y, Martinou JC, Marchetti P, Demaurex N, Wollheim CB (2008) Selective actions of mitochondrial fission/fusion genes on metabolism-secretion coupling in insulin-releasing cells. J Biol Chem 283:33347–33356 [PubMed: 18832378]

Pasqua T, Mahata S, Bandyopadhyay GK, Biswas A, Perkins GA, Sinha Hikim AP, Goldstein DS, Eiden LE, Mahata SK (2016) Impact of Chromogranin A deficiency on catecholamine storage, catecholamine granule morphology, and chromaffin cell energy metabolism in vivo. Cell Tissue Res 363:693–712 [PubMed: 26572539]

Putti R, Migliaccio V, Sica R, Lionetti L (2015) Skeletal muscle mitochondrial bioenergetics and morphology in high fat diet induced obesity and insulin resistance: focus on dietary fat source. Front Physiol 6:426 [PubMed: 26834644]

Ratti S, Curnis F, Longhi R, Colombo B, Gasparri A, Magni F, Manera E, Metz-Boutigue MH, Corti A (2000) Structure-activity relationships of chromogranin A in cell adhesion. Identification of an adhesion site for fibroblasts and smooth muscle cells. J Biol Chem 275:29257–29263 [PubMed: 10875933]

Sanchez-Margalet V, Gonzalez-Yanes C, Najib S, Santos-Alvarez J (2010) Metabolic effects and mechanism of action of the chromogranin A-derived peptide pancreastatin. Regul Pept 161:8–14 [PubMed: 20184923]

Santel A, Fuller MT (2001) Control of mitochondrial morphology by a human mitofusin. J Cell Sci 114:867–874 [PubMed: 11181170]

Santel A, Frank S, Gaume B, Herrler M, Youle RJ, Fuller MT (2003) Mitofusin-1 protein is a generally expressed mediator of mitochondrial fusion in mammalian cells. J Cell Sci 116:2763–2774 [PubMed: 12759376]

Smith CB, Eiden LE (2012) Is PACAP the major neurotransmitter for stress transduction at the adrenomedullary synapse? J Mol Neurosci 48:403–412 [PubMed: 22610912]

Soejima A, Inoue K, Takai D, Kaneko M, Ishihara H, Oka Y, Hayashi JI (1996) Mitochondrial DNA is required for regulation of glucose-stimulated insulin secretion in a mouse pancreatic beta cell line, MIN6. J Biol Chem 271:26194–26199 [PubMed: 8824267]

Stroth N, Kuri BA, Mustafa T, Chan SA, Smith CB, Eiden LE (2013) PACAP controls adrenomedullary catecholamine secretion and expression of catecholamine biosynthetic enzymes at high splanchnic nerve firing rates characteristic of stress transduction in male mice. Endocrinology 154:330–339 [PubMed: 23221599]

Tang K, Pasqua T, Biswas A, Mahata S, Tang J, Tang A, Bandyopadhyay GK, Sinha-Hikim AP, Chi NW, Webster NJ, Corti A, Mahata SK (2017) Muscle injury, impaired muscle function and insulin resistance in Chromogranin A-knockout mice. J Endocrinol 232:137–153 [PubMed: 27799464]

Tatemoto K, Efendic S, Mutt V, Makk G, Feistner GJ, Barchas JD (1986) Pancreastatin, a novel pancreatic peptide that inhibits insulin secretion. Nature 324:476–478 [PubMed: 3537810]

Taupenot L, Harper KL, Mahapatra NR, Parmer RJ, Mahata SK, O'Connor DT (2002) Identification of a novel sorting determinant for the regulated pathway in the secretory protein chromogranin A. J Cell Sci 115:4827–4841 [PubMed: 12432071]

Tondera D, Grandemange S, Jourdain A, Karbowski M, Mattenberger Y, Herzig S, Da Cruz S, Clerc P, Raschke I, Merkwirth C, Ehses S, Krause F, Chan DC, Alexander C, Bauer C, Youle R, Langer T, Martinou JC (2009) SLP-2 is required for stress-induced mitochondrial hyperfusion. EMBO J 28:1589–1600 [PubMed: 19360003]

Tota B, Angelone T, Mazza R, Cerra MC (2008) The chromogranin A-derived vasostatins: new players in the endocrine heart. Curr Med Chem 15:1444–1451 [PubMed: 18537621]

Tota B, Gentile S, Pasqua T, Bassino E, Koshimizu H, Cawley NX, Cerra MC, Loh YP, Angelone T (2012) The novel chromogranin A-derived serpinin and pyroglutaminated serpinin peptides are positive cardiac beta-adrenergic-like inotropes. FASEB J 26: 2888–2898 [PubMed: 22459152]

Tsuruzoe K, Araki E, Furukawa N, Shirotani T, Matsumoto K, Kaneko K, Motoshima H, Yoshizato K, Shirakami A, Kishikawa H, Miyazaki J, Shichiri M (1998) Creation and characterization of a mitochondrial DNA-depleted pancreatic beta-cell line: impaired insulin secretion induced by glucose, leucine, and sulfonylureas. Diabetes 47:621–631 [PubMed: 9568696]

Varndell IM, Lloyd RV, Wilson BS, Polak JM (1985) Ultrastructural localization of chromogranin: a potential marker for the electron microscopical recognition of endocrine cell secretory granules. Histochem J 17:981–992 [PubMed: 4066407]

Wai T, Langer T (2016) Mitochondrial dynamics and metabolic regulation. Trends Endocrinol Metab 27:105–117 [PubMed: 26754340]

Westermann B (2012) Bioenergetic role of mitochondrial fusion and fission. Biochim Biophys Acta 1817:1833–1838 [PubMed: 22409868]

Wilson BS, Lloyd RV (1984) Detection of chromogranin in neuroendocrine cells with a monoclonal antibody. Am J Pathol 115:458–468 [PubMed: 6375394]

Winkler H, Fischer-Colbrie R (1992) The chromogranins A and B: the first 25 years and future perspectives. Neuroscience 49:497–528 [PubMed: 1501763]

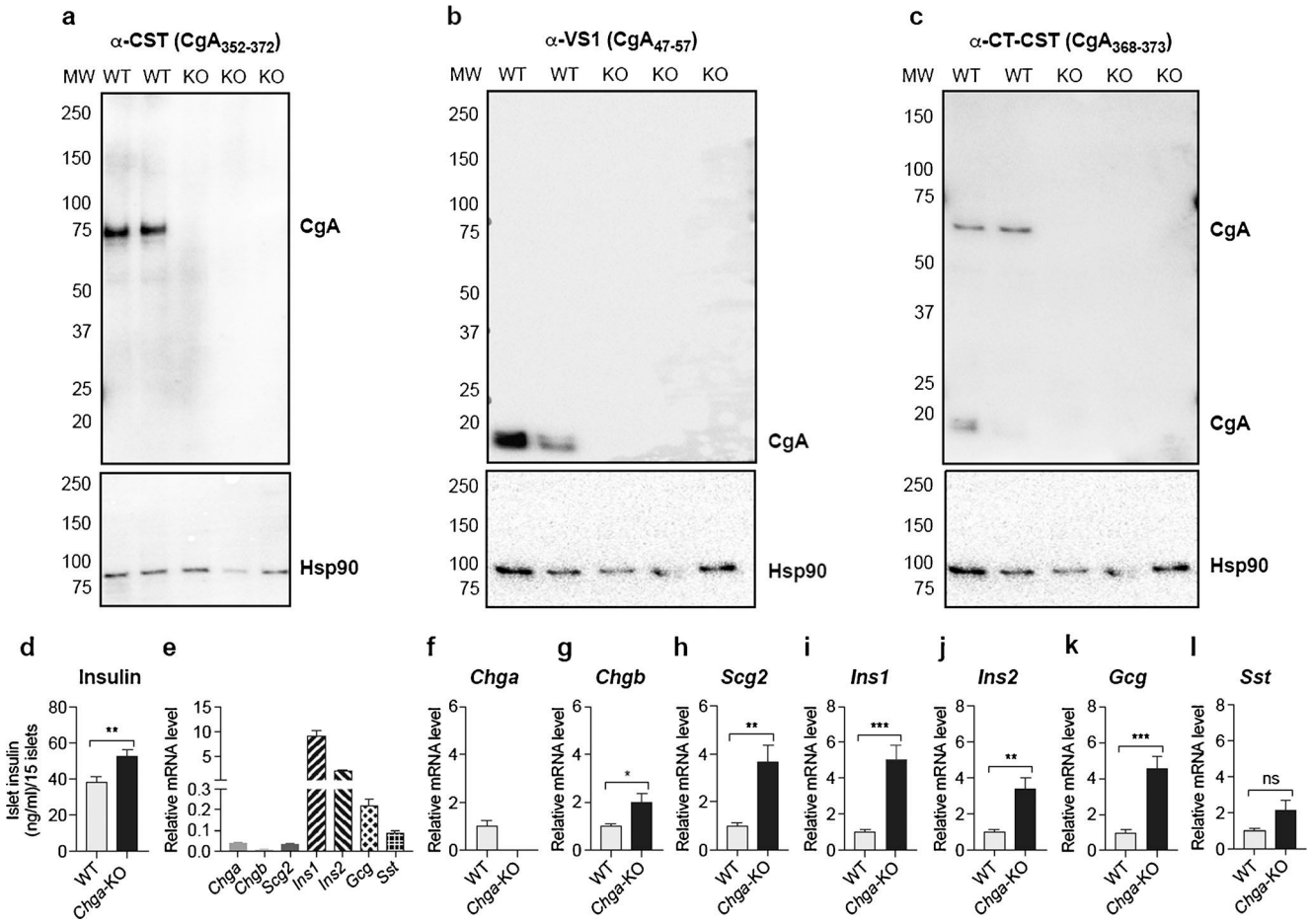

Fig. 1.

CgA is expressed in murine pancreatic islets and influences the vesicular quanta. **a–c** Western blot data showing expression of intact and processed CgA: **a** western blot with a polyclonal CST antibody (human $CgA_{352–372}$) showing a ~75-kDa band in WT mice that was absent in Chga-KO mice; **b** western blot with a monoclonal α-VS1 antibody (human $CgA_{47–57}$) showing an ~18-kDa band in WT mice that was absent in *Chga*-KO mice; **c** western blot with a polyclonal α-CT-CST antibody (human $CgA_{368–373}$) showing 2 CST-containing CgA bands: a ~65-kDa band and a ~20-kDa band in WT mice, which were absent in *Chga*-KO mice. **d** Intra-islet insulin concentration. qRT-PCR data showing mRNA levels of vesicular proteins ($n = 6$). **e** Basal expression in WT islets; **f** *Chga* mRNA levels in WT and *Chga*-KO islets; **g** *Chgb* mRNA levels in WT and *Chga*-KO islets; **h** *Scg2* mRNA levels in WT and *Chga*-KO islets; **i** *Ins1* mRNA levels in WT and *Chga*-KO islets; **j** *Ins2* mRNA levels in WT and *Chga*-KO islets; **k** *Gcg* mRNA levels in WT and *Chga*-KO islets; **l** *Sst* mRNA levels in WT and *Chga*-KO islets. *KO Chga*-KO, *MW* molecular weight, *WT* wild-type. *$P < 0.05$; **$P < 0.01$; ***: $P < 0.001$

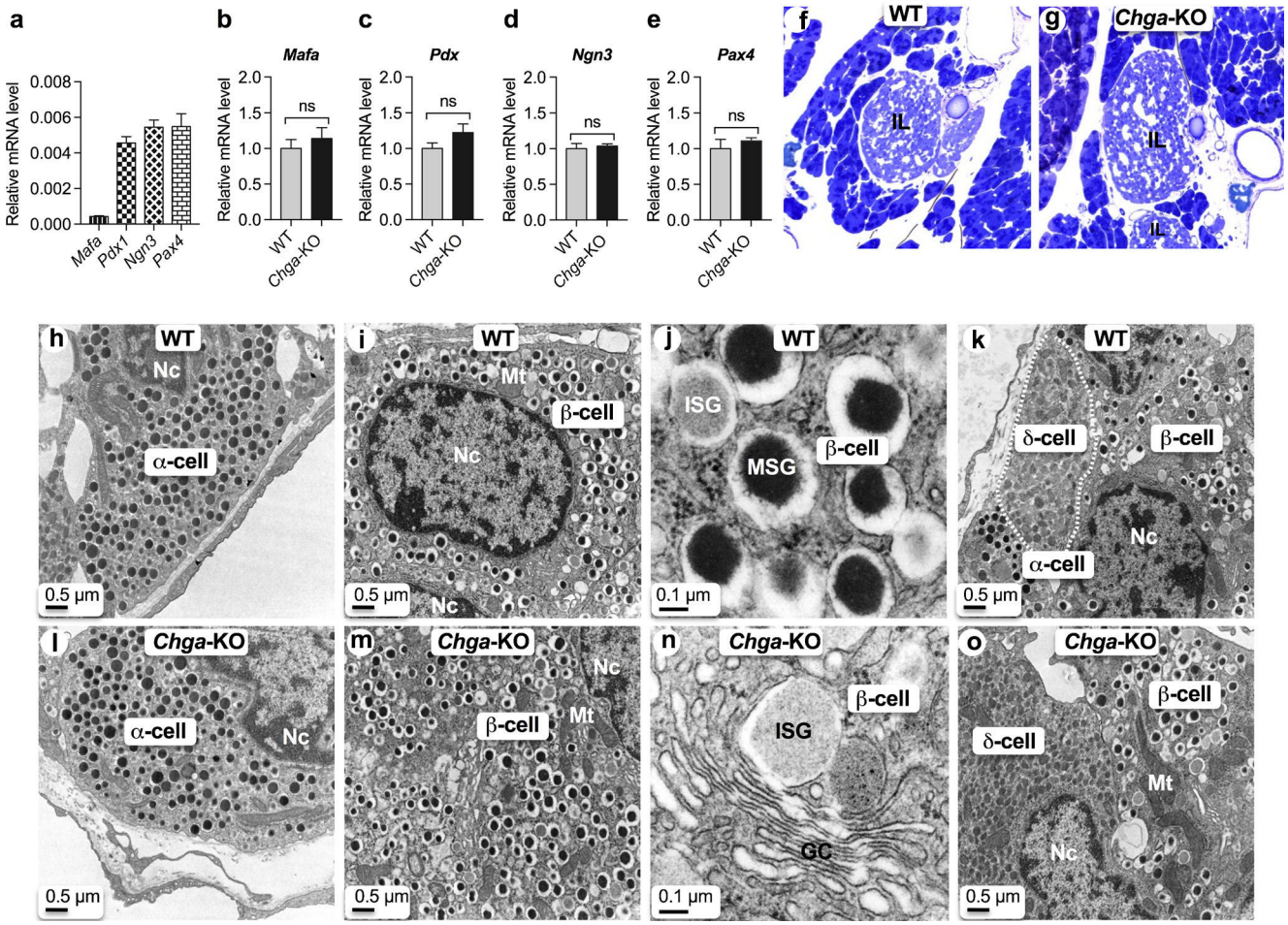

Fig. 2.

CgA does not influence ontogenesis and differentiation of pancreatic islets. qRT-PCR data showing expression of transcription factor genes ($n = 6$). **a** Basal expression in WT islets; **b** *Mafa* mRNA levels in WT and *Chga*-KO islets; **c** *Pdx1* mRNA levels in WT and *Chga*-KO islets; **d** *Ngn3* mRNA levels in WT and *Chga*-KO islets; **e** *Pax4* mRNA levels in WT and *Chga*-KO islets. **f, g** Toluidine blue-stained section of pancreatic islets: **f** WT; **g** *Chga*-KO. **h–o** Transmission electron microscopic (TEM) images of the pancreatic islets: **h** *α*-cell in WT islet; **i** *α*-cell in *Chga*-KO islet; **j** β-cell in WT islet; **k** β-cell in *Chga*-KO islet; **l** higher magnification images of a β-cell showing ISG and MSG; **m** higher magnification images of a β-cell showing Golgi complex and budding off an ISG from the middle of a Golgi stack; **n** β- and δ-cells (marked by *white dotted line*) in WT islet; **o** β- and δ-cells (marked by *dotted line*) in WT islet. *GC* Golgi complex, *ISG* immature secretory granule, *MSG* mature secretory granule, *Mt* mitochondria, *Nc* nucleus, *ns* not significant

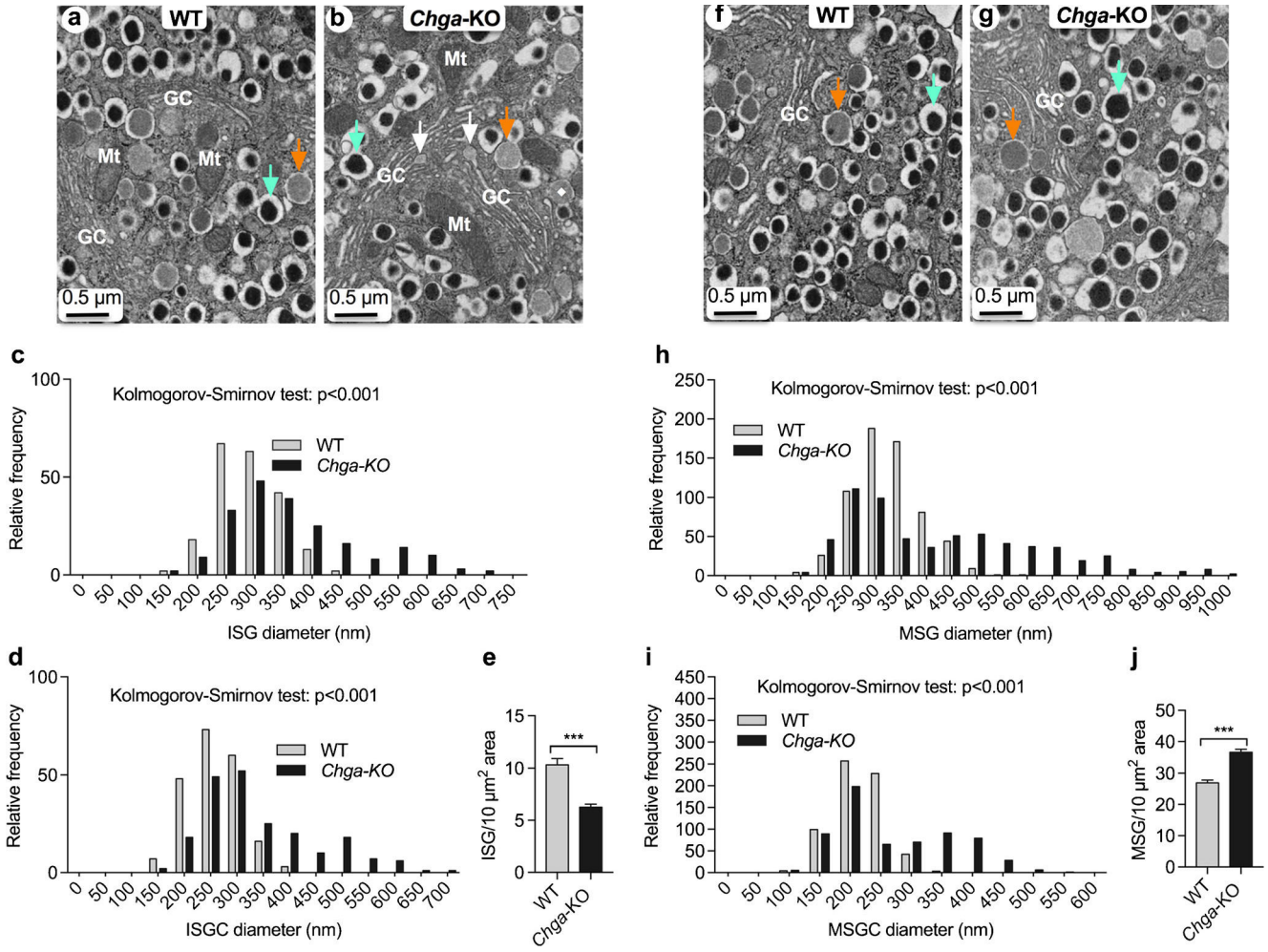

Fig. 3.

Analysis of α, β and δ-cell vesicular structure in pancreatic islets. TEM images of β-cells and morphometric analyses (620 vesicles from 4 mice each of the WT and *Chga*-KO mice) of ISG and MSG. **a, b** TEM images of a β-cell: **a** WT islets; **b** *Chga*-KO islets. *Orange arrow* points to an ISG and *green arrow* points to a MSG. *White arrows* indicate the formation of ISGs at the tip of a Golgi stack. Morphometric analyses of ISG (250 vesicles from 4 mice each of the WT and *Chga*-KO mice). **c, d** Distribution of ISG diameter (**c**) and ISGC diameter (**d**) in WT and *Chga*-KO islets. **e** Abundance of ISGs in WT and *Chga*-KO islets. **f, g** TEM images of a β-cell: **f** WT island and **g** *Chga*-KO island where *orange arrow* points to an ISG and *green arrow* points to a MSG. Morphometric analyses (650 vesicles from 4 mice each of the WT and *Chga*-KO mice). **h, i** Distribution of MSG diameters (**h**) and MSGC diameter (**i**) in WT and *Chga*-KO islets. **j** Abundance of MSGs in WT and *Chga*-KO islets. *MSG* mature secretory granule, MSGC dense core of MSG, *GC* Golgi complex, *ISG* immature secretory granule, *ISGC* light core of ISG, *Mt* mitochondria. *** $P <$ 0.001

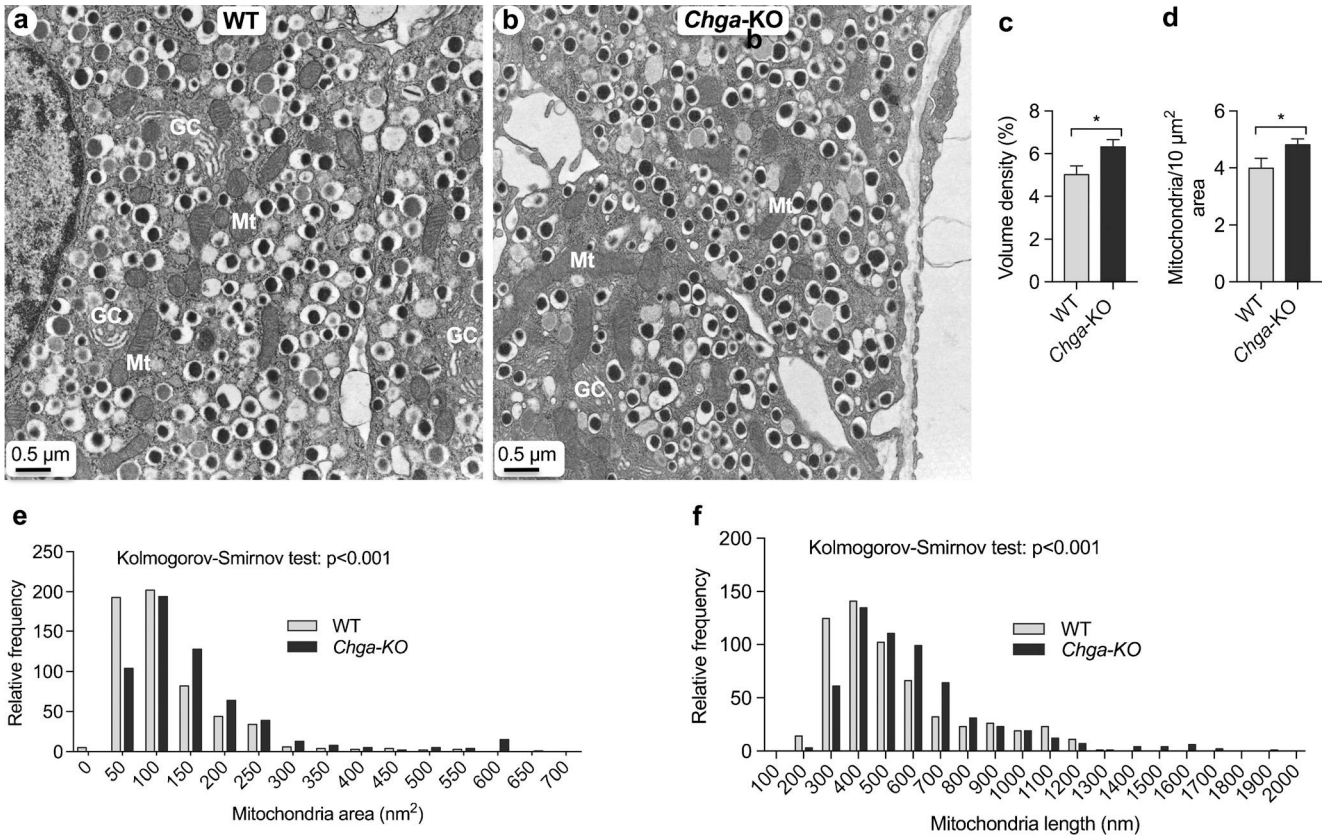

Fig. 4.

CgA influences mitochondrial morphology and abundance in β-cells. **a, b** TEM photographs of β-cells: **a** WT island; **b** *Chga*-KO island. **c, d** Morphometric analyses of mitochondria in β-cells: **c** volume density (60 images from 4 mice each of the WT and *Chga*-KO mice); **d** relative abundance of mitochondria (60 images from 4 mice each of the WT and *Chga*-KO mice). **e** Relative frequency of mitochondria area (650 mitochondria from 4 mice each of the WT and *Chga*-KO mice). **f** Relative frequency of mitochondria length (650 mitochondria from 4 mice each of the WT and *Chga*-KO mice). *Mt* mitochondria. $*P < 0.05$

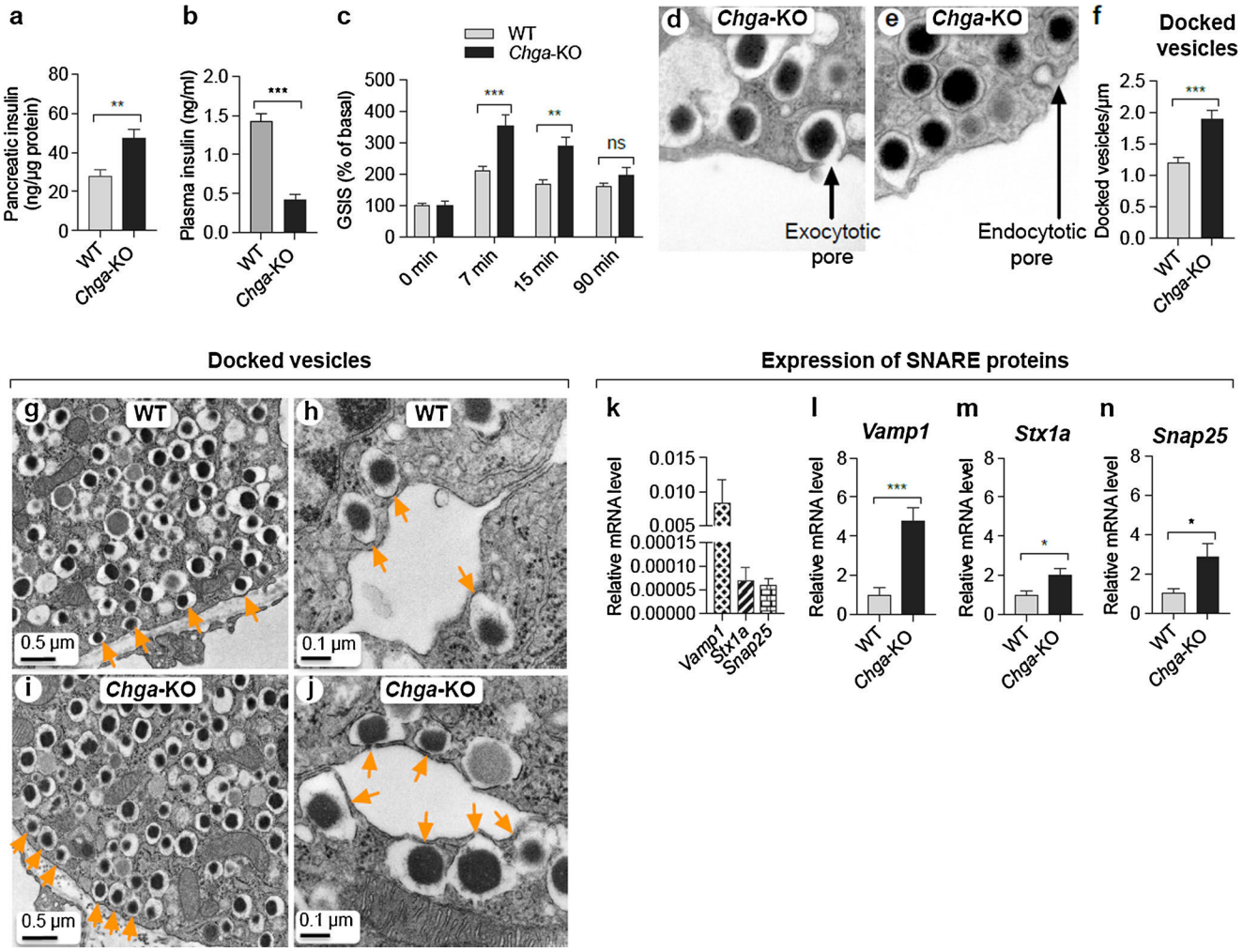

Fig. 5.

Loss of CgA leads to augmented exocytosis and elevated GSIS. **a** Pancreatic insulin content in WT and *Chga*-KO mice ($n = 10$). **b** Fasting basal plasma insulin in WT and *Chga*-KO mice ($n = 10$). **c** GSIS in WT and *Chga*-KO mice ($n = 10$). Two-way ANOVA: interaction, $P < 0.003$; time, $P < 0.001$; genotype, $P < 0.001$. **d, e** TEM images of β-cells: **d** exocytotic pore; **e** endocytotic vesicle. **f** Number of docked vesicles in WT and *Chga*-KO islets. **g–j** TEM images of β-cells: **g** low-magnification image of WT β-cell; **h** high-magnification image of WT β-cell; **i** low-magnification image of *Chga*-KO β-cell; **j** high-magnification image of *Chga*-KO β-cell. *Orange arrows* indicate docked vesicles. **k–n** qRT-PCR data showing mRNA levels of SNARE proteins: **k** basal expression of SNARE proteins; **l** *Vamp* mRNA levels in WT and *Chga*-KO islets; **m** *Stx1a* mRNA levels in WT and *Chga*-KO mice; **n** *Snap25* mRNA levels in WT and *Chga*-KO mice. *$P < 0.05$; **$P < 0.01$; ***$P < 0.001$

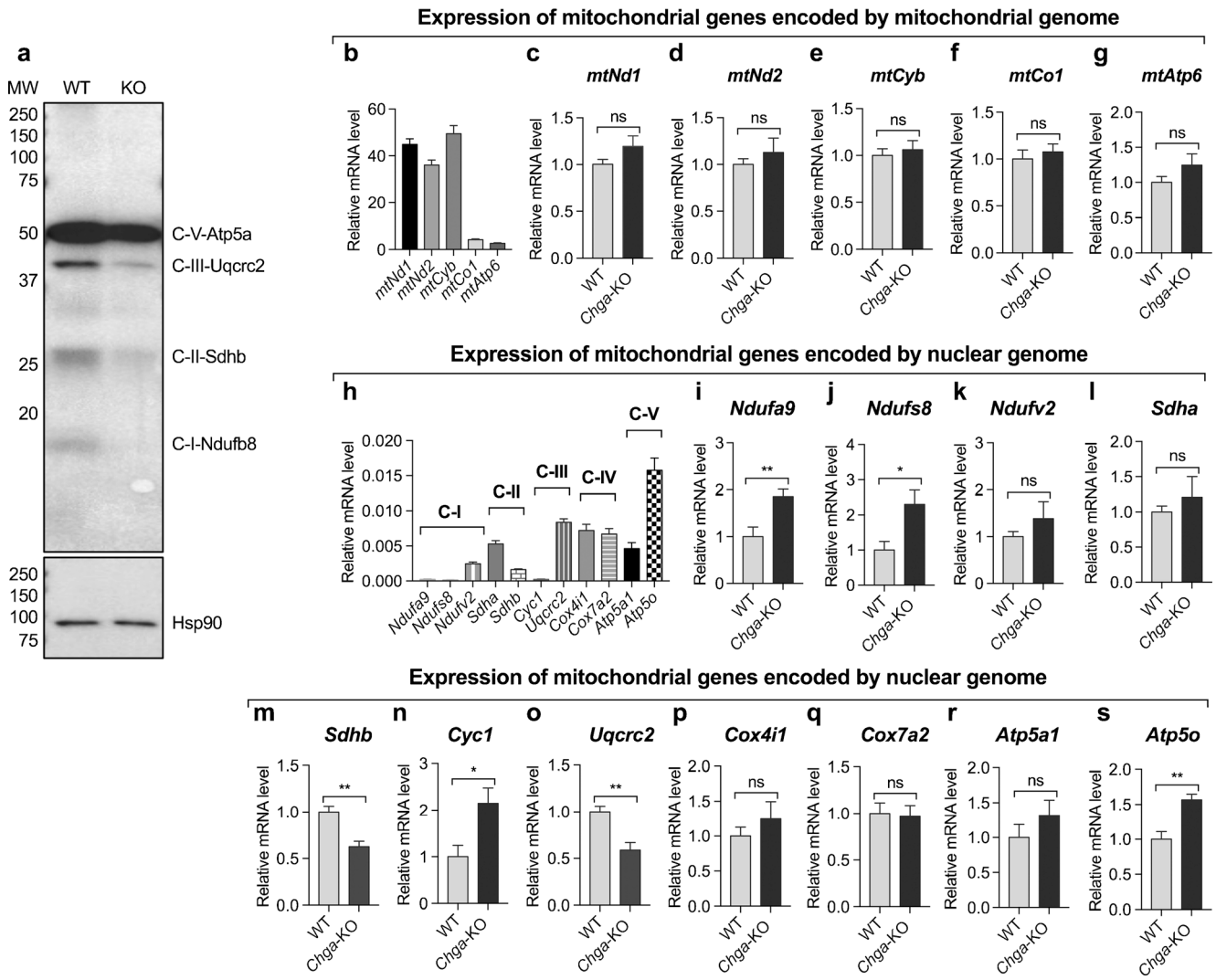

Fig. 6.

CgA modulates expression of genes regulating mitochondrial function. **a** Western blot showing expression of mitochondrial complex proteins. qRT-PCR data showing expression of genes encoded by mitochondrial and nuclear genomes. **b–g** Expression of genes encoded by mitochondrial genome: **b** basal mRNA levels of mitochondrial genes; **c** *mtNd1* mRNA levels in WT and *Chga*-KO islets; **d** *mtNd2* mRNA levels in WT and *Chga*-KO islets; **e** *mtCyb* mRNA levels in WT and *Chga*-KO islets; **f** *mtCo1* mRNA levels in WT and *Chga*-KO islets; **g** *mtAtp6* mRNA levels in WT and *Chga*-KO islets. **h–s** Expression of genes encoded by nuclear genomes: **h** basal expression of nuclear encoded genes in WT islets; **i** *Ndufa9* mRNA levels in WT and *Chga*-KO mice; **j** *Ndufs8* mRNA levels in WT and *Chga*-KO mice; **k** *Ndufv2* mRNA levels in WT and *Chga*-KO mice; **l** *Sdha* mRNA levels in WT and *Chga*-KO mice; **m** *Sdhb* mRNA levels in WT and *Chga*-KO mice; **n** *Cyc1* mRNA levels in WT and *Chga*-KO islets; **o** *Uqcrc2* mRNA levels in WT and *Chga*-KO islets; **p** *Cox4i1* mRNA levels in WT and *Chga*-KO islets; **q** *Cox7a2* mRNA levels in WT and *Chga*-KO islets; **r** *Atp5a1* mRNA levels in WT and *Chga*-KO islets; **s** *Atp5o* mRNA levels in WT and *Chga*-KO islets. **P* < 0.05; ***P* < 0.01

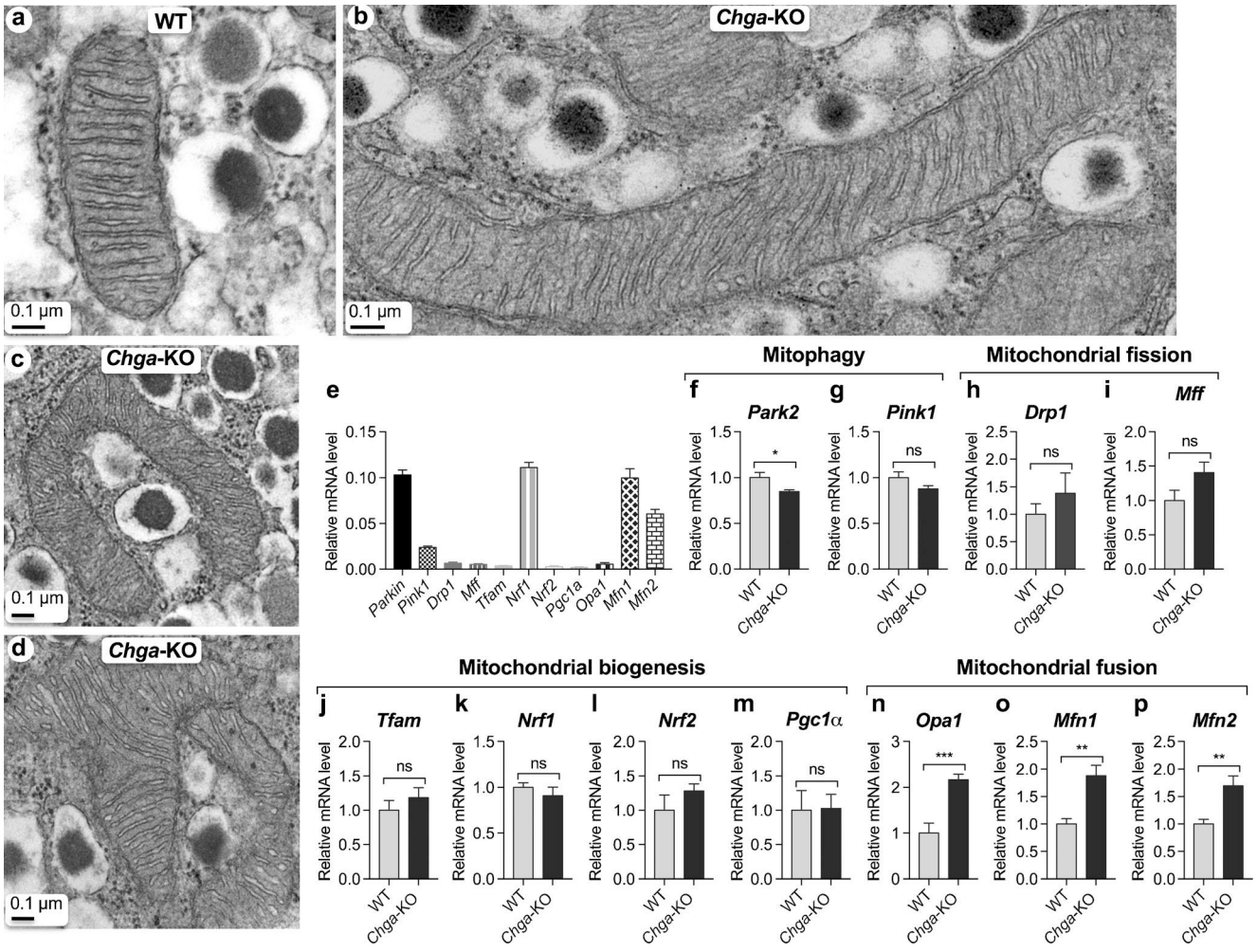

Fig. 7.

Chga-null islets display altered mitochondrial dynamics. **a–d** TEM images showing mitochondria in β-cells: **a** witochondria in WT island; **b** mitochondria in *Chga*-KO island; **c** mitochondrion in *Chga*-KO island showing fusion of 3 mitochondria; **d** mitochondria in *Chga*-KO island showing fusion of 4 mitochondria. **e–q** qRT-PCR showing expression of genes involved in mitochondrial dynamics: **e** basal expression in WT islets; **f** *Park2* mRNA levels in WT and *Chga*-KO islets; **g** *Pink1* mRNA levels in WT and *Chga*-KO islets; **h** *Drp1* mRNA levels in WT and *Chga*-KO islets; **i** *Mff* mRNA levels in WT and *Chga*-KO islets; **j** *Tfam* mRNA levels in WT and *Chga*-KO islets; **k** *Nrf1* mRNA levels in WT and *Chga*-KO islets; **l** *Nrf2* mRNA levels in WT and *Chga*-KO islets; **m** *Pgc1α* mRNA levels in WT and *Chga*-KO islets; **n** *Opa1* mRNA levels in WT and *Chga*-KO islets; **o** *Mfn1* mRNA levels in WT and *Chga*-KO islets; **p** *Mfn2* mRNA levels in WT and *Chga*-KO islets. *$P < 0.05$; **$P < 0.01$; ***$P < 0.001$

Table 1

Primer sequences for genes used in the real-time PCR analysis

Description	Sequence 5'-3'
Atp5a1-FP	TCTCCATGCCTCTAACACTCG
Atp5a1-FP	CCAGGTCAACAGACGTGTCAG
Atp5o-FP	TCTCGACAGGTTCGGAGCTT
Atp5o-RP	TTGACGGTGCGCTTGATGTAG
Chga-FP	CCAAGGTGATGAAGTGCGTC
Chga-RP	GGTGTCGCAGGATAGAGAGGA
Chgb-FP	AGCTCCAGTGGATAACAGGGA
Chgb-RP	GATAGGGCATTTGAGAGGACTTC
Cox4i1-FP	ATTGGCAAGAGAGCCATTTCTAC
Cox4i1-RP	TGGGGAAAGCATAGTCTTCACT
Cox7a2-FP	GCTGGCCCTTCGTCAGATT
Cox7a2-RP	GGCATCCCATTATCCTCCTGAA
Drp1-FP	CCTCAGATCGTCGTAGTGGGA
Drp1-RP	GTTCCTCTGGGAAGAAGGTCC
Gapdh-FP	AGGTCGGTGTGAACGGATTTG
Gapdh-RP	TGTAGACCATGTAGTTGAGGTCA
Gcg-FP	TGAATGAAGACAAACGCCACT
Gcg-RP	CCACTGCACAAAATCTTGGGC
Ins1-FP	CACTTCCTACCCCTGCTGG
Ins1-RP	ACCACAAAGATGCTGTTTGACA
Ins2-FP	GCTTCTTCTACACACCCATGTC
Ins2-RP	AGCACTGATCTACAATGCCAC
Mafa-FP	AGGAGGAGGTCATCCGACTG
Mafa-RP	CTTCTCGCTCTCCAGAATGTG
Mf-FP	ATGCCAGTGTGATAATGCAAGT
Mff-RP	CTCGGCTCTCTTCGCTTTG
Mfn1-FP	ATGGCAGAAACGGTATCTCCA
Mfn1-RP	GCCCTCAGTAACAAACTCCAGT
Mfn2-FP	AGAACTGGACCCGGTTACCA
Mfn2-RP	CACTTCGCTGATACCCCTGA
Mt-Atp6-FP	CCACACACCAAAAGGACGAACATGA
Mt-Atp6-RP	CGGACTGCTAATGCCATTGGTTG
Mt-Co1-FP	CACTACCAGTGCTAGCCGCA
Mt-Co1-RP	TCCTGGGAGGATAAGAATATAAACTTCT
Mt-Cyb-FP	CTTTGGGTCCCTTCTAGGAGTCTG
Mt-Cyb-RP	GCTGTGGCTATGACTGCGAACAG
Mt-Nd1-FP	TGCACCTACCCTATCACTC
Mt-Nd1-RP	ATTGTTTGGGCTACGGCTC
Ndufa9-FP	GTCCGCTTTCGGGTTGTTAGA

Description	Sequence 5'-3'
Ndufa9-RP	CCTCCTTTCCCGTGAGGTA
Ndufs8-FP	GTGGCGGCAACGTACAAGTAT
Ndufs8-RP	GAATCCGAGCTGCATTGTCAG
Ndufv2-FP	GCAAGGAATTTGCATAAGACAGC
Ndufv2-RP	TAGCCATCCATTCTGCCTTTG
Ngn3-FP	CCAAGAGCGAGTTGGCACT
Ngn3-RP	CGGGCCATAGAAGCTGTGG
Nrf1-FP	AGCACGGAGTGACCCAAAC
Nrf1-RP	AGGATGTCCGAGTCATCATAAGA
Nrf2-FP	CTTTAGTCAGCGACAGAAGGAC
Nrf2-RP	AGGCATCTTGTTTGGGAATGTG
Opa1-FP	TGGAAAATGGTTCGAGAGTCAG
Opa1-RP	CATTCCGTCTCTAGGTTAAAGCG
Parkin-FP	GAGGTCGATTCTGACACCAGC
Parkin-RP	CCGGCAAAAATCACACGCAG
Pax4-FP	GCAGTGTGAATCAGCTAGGGG
Pax4-RP	CAGGGTCGCATCCCTCTTATT
Pdx1-FP	CCCCAGTTTACAAGCTCGCT
Pdx1-RP	CTCGGTTCC ATTCGGGAAAGG
Pink1-FP	TTCTTCCGCCAGTCGGTAG
Pink1-RP	CTGCTTCTCCTCGATCAGCC
Scg2-FP	GGAGCTAAGGCGTACCGAC
Scg2-RP	TGGACATTCTCCAATCTGAGGT
Sdha-FP	GGAACACTCCAAAAACAGACCT
Sdha-RP	CCACCACTGGGTATTGAGTAGAA
Sdhb-FP	ATTTACCGATGGGACCCAGAC
Sdhb-RP	GTCCGCACTTATTCAGATCCAC
Snap25-FP	GCAAGGCGAACAACTGGAAC
Snap25-RP	GGCCACTACTCCATCCTGATT
Sst-FP	CCACCGGGAAACAGGAACTG
Sst-RP	TTGCTGGGTTCGAGTTGGC
Stx1a-FP	AAGATTGCCGAAAACGTGGAG
Stx1a-RP	TGCTCAATGCTCTTTAGCTTGG
Tfam-FP	ATTCCGAAGTGTTTTTCCAGCA
Tfam-RP	TCTGAAAGTTTTGCATCTGGGT
Uqcrc2-FP	AAAGTTGCCCCGAAGGTTAAA
Uqcrc2-RP	GAGCATAGTTTTCCAGAGAAGCA
Vamp1-FP	CATGCGTGTGAATGTGGACAA
Vamp1-RP	GATGGCACAGATAGCTCCCAG